Journal of Inorganic and Organometallic Polymers and Materials (2024) 34:3178–3190
https://doi.org/10.1007/s10904-024-03180-7

RESEARCH

Cationic Iridium(III) Complexes Bearing Different Bulky N,N′-Chelating Ligands

Wai-Yeung Wong[1,2,3,4] · Nga-Yuen Chau[2] · Qiwei Wang[1,2] · Lu Jiang[1] · Junlong Li[1] · Zelin Sun[3,4]

Received: 3 June 2024 / Accepted: 6 June 2024 / Published online: 25 June 2024

Abstract

Six cationic iridium(III) complexes bearing different bulky N,N′-chelating ligands were successfully synthesized and characterized by spectroscopic, electrochemical, thermal and photophysical methods. Because the molecular quenching and self-aggregation within molecules would deteriorate the device efficiency, the bulky molecules can suppress these problems and improve the device performance. The best doped organic light-emitting diodes based on these charged Ir(III) complex **E1** exhibited L_{max} of 26,800 cd/m^2, $\eta_{L,\,max}$ of 35.0 cd/A and $\eta_{P,\,max}$ of 18.5 lm/W, which also showed a small efficiency roll-off in the range of 100 to 1000 cd/m^2.

Graphical Abstract

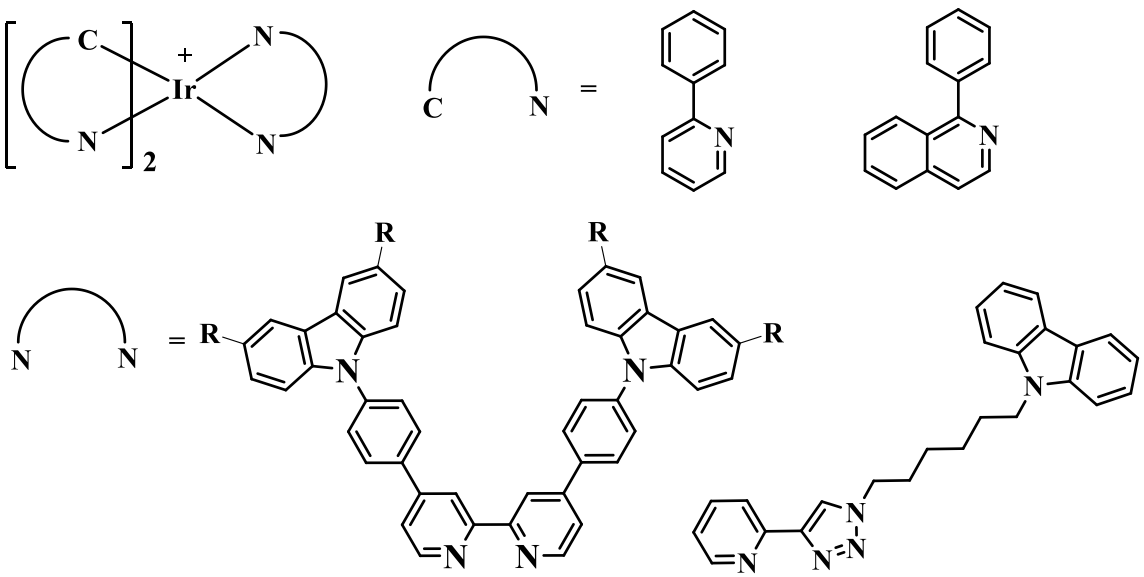

Keywords Iridium · Cationic complexes · Synthesis · Phosphorescence · Organic light-emitting devices

✉ Wai-Yeung Wong
wai-yeung.wong@polyu.edu.hk

✉ Qiwei Wang
wqw@cioc.ac.cn

[1] Antibiotics Research and Re-evaluation Key Laboratory of Sichuan Province, Sichuan Industrial Institute of Antibiotics, Chengdu University, Chengdu 610052, People's Republic of China

[2] Department of Chemistry, Hong Kong Baptist University, Waterloo Road, Kowloon Tong, Hong Kong, People's Republic of China

[3] Department of Applied Biology and Chemical Technology, The Hong Kong Polytechnic University (PolyU), Hung Hom, Hong Kong, People's Republic of China

[4] PolyU Shenzhen Research Institute, Shenzhen 518057, People's Republic of China

1 Introduction

Nowadays, some highly efficient organic light-emitting diodes have been successfully developed [1, 2]. Plenty of research works have been inevitably focused on the neutral metal complexes since these molecules are easily sublimable and compatible with the hydrophobic matrices employed in device fabrication [3, 4]. On the subject of charged metal complexes, their poor sublimability and the compatibility with hydrophobic hosts should be taken into consideration for their OLED fabrication. In any case, the charged compounds could exhibit good charge-transporting properties as well as good solubility in polar solvents. The power consumed by these OLED devices could be relatively low even by applying inert metal electrodes. In addition, their exquisite redox stability could notably improve the device stability.

In the past, many diimine ligands have been utilized for investigating the luminescence properties of the Ru(II) and Ir(III) complexes: 2,2′-bipyridine (bpy), 1,10-phenanthroline (phen) and (pyrazolyl)pyridine, to name but a few [5–7]. The N^N bipyridines are commonly used as ancillary ligand in the charged compounds since they occupy the low-energy π^*-orbitals in the transition [8].

In this study, neutral 2,2′-bipyridine-based and 2-pyridylazole-based bidentate chelates act as ancillary ligand for these charged iridium(III) complexes. To our understanding, the light-emitting molecules aggregate within the emissive layer causing triplet–triplet annihilation (TTA). This phenomenon has an impact on the OLED performance [9, 10]. In view of reducing the aggregation and π–π stacking between molecules, we introduced two carbazole moieties into the neutral 2,2′-bipyridine to afford two bulky N^N ligands **L1** and **L2**.

Besides, Su et al. demonstrated that the cationic iridium(III) complexes bearing ancillary ligands with a phenothiazine or a carbazole end-capped alkyl groups exhibited aggregation-induced emission (AIE) properties [11, 12]. Since aggregation-caused quenching (ACQ) influences the optical device applications, these AIE-active complexes could overcome this problem effectively. Complexes with 1,2,4-triazole moiety have been developed whereas such iridium(III) complexes based on 1,2,3-triazole are much less explored. In this study, we designed another N^N ligand, 9-(6-(4-(pyridin-2-yl)-1*H*-1,2,3-triazol-1-yl)hexyl)-9*H*-carbazole **L3** for the same rationale. This ligand with a carbazole end-capped hexyl group could reduce the intermolecular π–π stacking in the solid state. It is hoped that the iridium(III) complexes possessing this ligand will also show the AIE behavior, which is beneficial to their electroluminescent performance.

2 Experimental Section

2.1 Materials and Instruments

All the chemicals were purchased from Acros or Aldrich and used as received unless otherwise specified. THF was dried by distillation from sodium with benzophenone as an indicator under a nitrogen atmosphere. Separation and purification of products were achieved by column chromatography on silica gel. TLC was carried out in air using laboratory grade solvents as eluents.

The positive-ion fast atom bombardment (FAB) mass spectra were recorded in *m*-nitrobenzyl alcohol matrices on a Finngin-MAT SSQ710 mass spectrometer. Infrared spectra were recorded on the Nicolet Magna 550 Series II FTIR spectrometer, using KBr pellets for solid state spectroscopy. NMR spectra were measured in deuterated solvents as the lock and reference on Varian INOVA 400 instrument or Bruker AV 400 MHz FT-NMR spectrometer, with ^{1}H and ^{13}C NMR chemical shifts quoted relative to Me_4Si standard and ^{31}P chemical shifts relative to an 85% H_3PO_4 external reference. Electronic absorption spectra were obtained with a Hewlett Packard 8453 spectrometer. Solution state photoluminescence measurements were obtained by the LS50B fluorescent spectrometer. For lifetime measurements, the third harmonics, 355 nm line of a Q-switched Nd:YAG laser was used as the excitation light source. The emission was recorded by using a PMT and a HP54522A 500 MHz oscilloscope. The PL spectra were measured in CH_2Cl_2 with a PTI Fluorescence Master Series QM1 spectrophotometer. Thermal analysis was performed with a Perkin-Elmer TGA6 thermal analyzer. The cyclic voltammograms were acquired with a CHI model 600D electrochemical station in deoxygenated acetonitrile containing 0.1 M $[Bu_4N]PF_6$ as the supporting electrolyte. A conventional three-electrode configuration consisting of a platinum working electrode, a Pt-wire counter electrode and a Ag/AgCl reference electrode was used. The polymer films were casted on the ITO covered glass. All potentials reported were quoted with reference to the ferrocene-ferrocenium (Fc/Fc^+) couple at a scan rate of 100 mV s^{-1}.

2.2 Preparation of Ligands

Due to their poor solubility in common d-solvents, the *N,N′*-ligands **L1** and **L2** could not be characterized by NMR spectrometry. They would be used for metal coordination directly.

2.2.1 Synthesis of L1

9-(4-Bromophenyl)-9*H*-carbazole was prepared as reported by the literature method [13]. The brominated compound (2.5 g, 7.758 mmol) was treated with 2.4 M *n*-BuLi

(3.5 ml, 8.534 mmol), followed by trimethylborate (2.6 ml, 0.023 mol). The (4-(9*H*-carbazol-9-yl)phenyl)boronic acid (1.2 g, 4.179 mmol) was refluxed with 4,4′-dibromopyridine (440 mg, 1.401 mmol) in a solution of tetrahydrofuran (40 ml) and aqueous 2 M Na_2CO_3 catalyzed by $Pd(PPh_3)_4$ (50 mg). A grey solid precipitated out in the course of reaction, which was filtered and washed with diethyl ether (78%).

2.2.2 Synthesis of L2

(4-(3,6-Di-*tert*-butyl-9*H*-carbazol-9-yl)phenyl)boronic acid was prepared using a similar method to that of **L1**. A mixture of (4-(3,6-di-*tert*-butyl-9*H*-carbazol-9-yl)phenyl) boronic acid (1.2 g, 3.005 mmol), 4,4′-dibromopyridine (315 mg, 1.002 mmol) and $Pd(PPh_3)_4$ (50 mg) was refluxed in toluene (40 ml) and 2 M Na_2CO_3 for 2 days. A pale grey powder was obtained (66%).

2.2.3 Synthesis of L3

Ligand **L3** was prepared from the "click" reaction. 9-(6-Bromohexyl)-9*H*-carbazole was formed by reacting carbazole (4.0 g, 0.024 mol) with 1,6-dibromohexane (5.5 ml, 0.036 mol). The brominated compound (2.0 g, 6.056 mmol) was heated with sodium azide (0.59 g, 9.076 mmol) in dimethylsulfoxide solution. A mixture of 9-(6-azidohexyl)-9*H*-carbazole (800 mg, 2.736 mmol), 2-ethynylpyridine (0.41 ml, 4.104 mmol), $CuSO_4.5H_2O$ (68 mg, 0.274 mmol) and sodium ascorbate (271 mg, 1.368 mmol) was stirred in dichloromethane (12 ml) and H_2O (9 ml) at room temperature. The ligand **L3** was obtained as a pale yellow solid (85%).

Spectral data: ^{1}H NMR ($CDCl_3$): δ (ppm) 8.58 (s, 1H, Ar), 8.14–8.12 (m, 1H, Ar), 8.09 (d, $J = 7.6$ Hz, 3H, Ar), 7.81–7.77 (m, 1H, Ar), 7.47–7.43 (m, 2H, Ar), 7.38 (d, $J = 8.0$ Hz, 2H, Ar), 7.24–7.20 (m, 3H, Ar), 4.36 (t, $J = 6.9$ Hz, 2H, CH_2), 4.30 (t, $J = 6.9$ Hz, 2H, CH_2), 1.92–1.87 (m, 4H, CH_2), 1.42–1.39 (m, 4H, CH_2). MS (MALDI-TOF): *m/z* 395.20 (M^+).

2.3 Preparation of Iridium(III) Complexes

General Procedures for the Synthesis of Cationic Iridium(III) Complexes: Iridium(III) chloro-bridged dimers $[(ppy)_2Ir(\mu\text{-}Cl)]_2$ (ppy = 2-phenylpyridine) and $[(piq)_2Ir(\mu\text{-}Cl)]_2$ (piq = 2-phenylisoquinoline) were prepared according to the literature procedure [17]. The iridium dimer was allowed to react with 2.5 molar equivalents of N,N′-chelating ligands in a solution of dichloromethane (10 ml) and methanol (5 ml), and the mixture was heated at 45 °C for 24 h. For anion exchange, an excess amount of sodium hexafluorophosphate was added and the mixture was stirred at room temperature. The charged iridium(III) complexes were purified by column chromatography with silica gel.

E1: Orange powder (36%).

Spectral data: ^{1}H NMR ($CDCl_3$): δ (ppm) 8.92 (s, 2H, Ar), 8.11 (d, $J = 7.6$ Hz, 4H, Ar), 8.06 (d, $J = 8.6$ Hz, 4H, Ar), 8.01 (d, $J = 5.8$ Hz, Ar, 2H), 7.48–7.45 (m, 4H, Ar), 7.73–7.70 (m, 6H, Ar), 7.58 (dd, $J_1 = 5.8$ Hz, $J_2 = 1.7$ Hz, 2H, Ar), 7.46 (d, $J = 8.2$ Hz, 4H, Ar), 7.38–7.34 (m, 4H, Ar), 7.28–7.24 (m, 4H, Ar), 7.14–7.10 (m, 2H, Ar), 7.09–7.05 (m, 2H, Ar), 6.99–6.95 (m, 2H, Ar), 6.37 (d, $J = 6.8$ Hz, 2H, Ar). ^{13}C NMR ($CDCl_3$): δ (ppm) 167.68, 156.41, 150.80, 150.52, 150.34, 149.11, 143.65, 140.36, 139.97, 138.12, 134.29, 131.86, 130.82, 129.27, 127.61, 126.18, 125.49, 124.75, 123.68, 123.09, 122.65, 120.37, 120.30, 119.53, 109.93. MS (MALDI-TOF): *m/z* 1284.3 (M^+).

E2: Orange powder (29%).

Spectral data: ^{1}H NMR ($CDCl_3$): δ (ppm) 8.91 (s, 2H, Ar), 8.11 (s, 4H, Ar), 8.05 (d, $J = 7.8$ Hz, 4H, Ar), 8.01 (d, $J = 5.8$ Hz, 2H, Ar), 7.91 (d, $J = 7.8$ Hz, 2H, Ar), 7.77–7.69 (m, 10H, Ar), 7.59–7.58 (m, 2H, Ar), 7.43–7.38 (m, 8H, Ar), 7.11 (t, $J = 6.8$ Hz, 2H, Ar), 7.05 (t, $J = 7.6$ Hz, 2H, Ar), 6.94 (t, $J = 7.4$ Hz, 2H, Ar), 6.37 (d, $J = 7.6$ Hz, 2H, Ar), 1.43 (s, 36H, Ar). ^{13}C NMR ($CDCl_3$): δ (ppm) 167.67, 156.38, 150.85, 150.58, 150.34, 149.10, 143.64, 143.36, 140.56, 138.70, 138.13, 133.67, 131.87, 130.81, 129.15, 127.09, 125.48, 124.75, 123.86, 123.76, 123.63, 122.86, 122.64, 119.51, 116.24, 109.42 (Ar), 34.75 (CH), 31.61 (CH_3). MS (MALDI-TOF): *m/z* 1508.6 (M^+).

E3: Yellow powder (29%).

Spectral data: ^{1}H NMR ($CDCl_3$): δ (ppm) 8.87 (s, 1H, Ar), 8.25 (d, $J = 8.0$ Hz, 1H, Ar), 8.11 (d, $J = 7.6$ Hz, 2H, Ar), 7.95–7.91 (m, 1H, Ar), 7.86 (d, $J = 8.1$ Hz, 1H, Ar), 7.74 (d, $J = 5.0$ Hz, 1H, Ar), 7.72–7.68 (m, 1H, Ar), 7.66–7.63 (m, 1H, Ar), 7.59 (d, $J = 8.1$ Hz, 1H, Ar), 7.49–7.45 (m, 2H, Ar), 7.43–7.37 (m, 5H, Ar), 7.25–7.19 (m, 3H, Ar), 7.03–6.99 (m, 1H, Ar), 6.98–6.95 (m, 1H, Ar), 6.91–6.87 (m, 2H, Ar), 6.86–6.80 (m, 2H, Ar), 6.28–6.25 (m, 2H, Ar), 4.37–4.34 (m, 2H, CH_2), 4.22–4.19 (m, 2H, CH_2), 1.85–1.81 (m, 2H, CH_2), 1.73–1.69 (m, 2H, CH_2), 1.14–1.07 (m, 4H, CH_2). MS (MALDI-TOF): *m/z* 1041.3 (M^+).

E4: Orange powder (36%).

Spectral data: ^{1}H NMR ($CDCl_3$): δ (ppm) 8.90 (s, 4H, Ar), 8.04 (d, $J = 8.0$ Hz, 2H, Ar), 7.98 (t, $J = 8.8$ Hz, 8H, Ar), 7.83–7.81 (m, 2H, Ar), 7.72 (d, $J = 5.8$ Hz, 2H, Ar), 7.69–7.65 (m, 4H, Ar), 7.60–7.55 (m, 6H, Ar), 7.43–7.41 (m, 2H, Ar), 7.38 (d, $J = 6.4$ Hz, 2H, Ar), 7.34 (d, $J = 8.2$ Hz, 4H, Ar), 7.25–7.21 (m, 4H, Ar), 7.16–7.12 (m, 4H, Ar), 7.10–7.06 (m, 4H, Ar), 6.89–6.85 (m, 2H, Ar), 6.30–6.28 (m, 2H, Ar). ^{13}C NMR ($CDCl_3$): δ (ppm) 168.95, 156.33, 153.82, 150.72, 150.34, 145.67, 140.66, 140.33, 139.90, 137.15, 134.22, 132.36, 131.68, 130.92, 130.71, 129.27, 128.69, 127.72, 127.55, 126.89, 126.36, 126.15, 125.45,

123.65, 123.05, 122.36, 122.23, 120.32, 120.24, 109.97 (Ar). MS (MALDI-TOF): *m/z* 1384.4 (M^+).

E5: Orange powder (31%).

Spectral data: ^{1}H NMR ($CDCl_3$): δ (ppm) 8.99–8.96 (m, 4H, Ar), 8.31 (d, J = 8.0 Hz, 2H, Ar), 8.11 (s, 4H, Ar), 8.08 (d, J = 8.6 Hz, 4H, Ar), 7.94–7.92 (m, 2H, Ar), 7.82 (d, J = 5.8 Hz, 2H, Ar), 7.79–7.75 (m, 8H, Ar), 7.67 (d, J = 6.4 Hz, 2H, Ar), 7.63–7.61 (m, 2H, Ar), 7.47 (d, J = 6.4 Hz, 2H, Ar), 7.44 (s, 8H, Ar), 7.17–7.13 (m, 2H, Ar), 6.96–6.92 (m, 2H, Ar), 6.38–6.36 (m, 2H, Ar), 1.45 (s, 36H, CH_3). ^{13}C NMR ($CDCl_3$): δ (ppm) 168.95, 156.35, 153.88, 150.90, 150.27, 145.66, 143.33, 140.70, 140.59, 138.70, 137016, 133.67, 132.38, 131.66, 130.90, 129.18, 128.66, 127.74, 127.10, 126.91, 126.37, 125.48, 123.85, 123.76, 123.02, 122.32, 122.22, 116.23, 109.44 (Ar), 34.75, 31.99 (CH_3). MS (MALDI-TOF): *m/z* 1608.6 (M^+).

E6: Orange powder (28%).

Spectral data: ^{1}H NMR ($CDCl_3$): δ (ppm) 8.93–8.91 (m, 2H, Ar), 8.82 (d, J = 8.7 Hz, 1H, Ar), 8.30–8.25 (m, 2H, Ar), 8.16 (d, J = 8.0 Hz, 1H, Ar), 8.06 (d, J = 7.6 Hz, 2H, Ar), 7.95–7.91 (m, 1H, Ar), 7.84–7.81 (m, 1H, Ar), 7.75–7.73 (m, 2H, Ar), 7.57–7.54 (m, 3H, Ar), 7.52–7.48 (m, 1H, Ar), 7.45–7.39 (m, 3H, Ar), 7.34–7.30 (m, 4H, Ar), 7.22–7.16 (m, 4H, Ar), 7.12–7.08 (m, 1H, Ar), 7.03–6.98 (m, 1H, Ar), 6.89–6.85 (m, 1H, Ar), 6.80–6.76 (m, 1H, Ar), 6.42–6.40 (m, 1H, Ar), 6.27–6.25 (m, 1H, Ar), 4.36–4.26 (m, 2H, CH_2), 4.14–4.04 (m, 2H, CH_2), 1.80–1.73 (m, 2H, CH_2), 1.58–1.51 (m, 2H, CH_2), 0.95–0.83 (m, 4H, CH_2). MS (MALDI-TOF): *m/z* 1141.3 (M^+).

3 Results and Discussion

3.1 Synthesis

Ligands **L1–L2** were synthesized from the reaction of 4,4′-dibromo-2,2′-bipyridine and their corresponding carbazole boronic acids. The brominated compounds were prepared via Ullmann coupling reaction between 1-bromo-4-iodobenzene and carbazole moieties using CuI/1,10-phen/NaOH as catalyst. With the treatment of *n*-butyllithium and trimethylborate, followed by 2 M HCl, they were subsequently transformed into the boronic acids. Finally, the N,N′-ligands **L1–L2** were obtained by coupling 4,4′-dibromo-2,2′-bipyridine with (4-(9*H*-carbazol-9-yl)phenyl)boronic acid and (4-(3,6-di-*tert*-butyl-9*H*-carbazol-9-yl)phenyl)boronic acid in the presence of a catalytic amount of $Pd(PPh_3)_4$ (Scheme 1). The ligands precipitated out in the course of reaction, which were purified by filtration and washed with ether solution.

Ligand **L3** can be prepared from the "click" reaction of alkynes and organic azides in good yield [14]. Firstly, the 9-(6-bromohexyl)-9*H*-carbazole was made by reacting carbazole with a stoichiometric amount of 1,6-dibromohexane. The brominated precursor was heated with sodium azide in dimethylsulfoxide solution to prepare the 9-(6-azidohexyl)-9*H*-carbazole.

As shown in Scheme 2, a slight excess amount of sodium ascorbate was used in the Cu(I)-catalyzed azide-alkyne cycloaddition reaction, which can prevent the oxidative homocoupling products formed and also act as a reducing agent [15]. The Cu(I)-acetylide intermediate was in situ generated from the reaction of 2-ethynylpyridine and copper(II) sulphate, which was promptly treated with the 9-(6-azidohexyl)-9H-carbazole at room temperature [16]. The intermediate formed would undergo cyclization, followed by hydrolysis of copper-carbon bond to afford the ligand **L3** in high yield. After filtration and washing with ethanol, the ligand could be used without further purification.

Iridium(III) chloro-bridged dimers were prepared according to the literature method [17]. The $[(ppy)_2Ir(\mu\text{-}Cl)]_2$ (ppy = 2-phenylpyridine) and $[(piq)_2Ir(\mu\text{-}Cl)]_2$ (piq = 2-phenylisoquinoline) were readily synthesized from the reaction of $IrCl_3.3H_2O$ and their cyclometalating ligands. The ligands prepared would react with the chloro-bridged Ir (III) dimers $[(C\text{^}N)_2Ir(\mu\text{-}Cl)]_2$ in a solution of dichloromethane and methanol (v/v, 2:1) under reflux overnight in the dark condition [18, 19]. Then, an excess amount of sodium hexafluorophosphate was added to the reaction mixture while swirling at room temperature to produce the compounds **E1–E6**. These charged compounds were purified by silica gel chromatography using dichloromethane as eluent (Scheme 3).

3.2 Photophysical Properties

In this photophysical study, only metal complexes **E1–E6** were subjected to UV–Vis absorption and photoluminescence spectroscopies. Their UV–Vis absorption spectra are shown in Fig. 1 and the data are summarized in Table 1. The absorption bands below 350 nm received contribution from spin-allowed π–π* transitions in the cyclometalating ligands. In these iridium(III) complexes, the weak and plateau-like bands are extended from 350 nm to longer wavelength that are suggestive of ^{1}MLCT (metal-to-ligand charge transfer), ^{3}MLCT and ^{3}π–π* transitions from the ligands. Apparently, compounds featuring N,N′-bipyridine ligands (**E1–E2** and **E4–E5**) showed a prominent peak at 350–455 nm.

The normalized PL spectra of compounds **E1–E6** in dichloromethane solution at 298 K and 77 K are presented in Figs. 2 and 3, respectively. Most complexes except **E3** emitted orange and red light at room temperature. For compound **E3**, it emitted blue-green light at room temperature. All compounds showed a broad and featureless emission peak. It is believed that these emissive excited states may result from the ^{3}MLCT or ^{3}LLCT transition [20, 21] (Fig. 4).

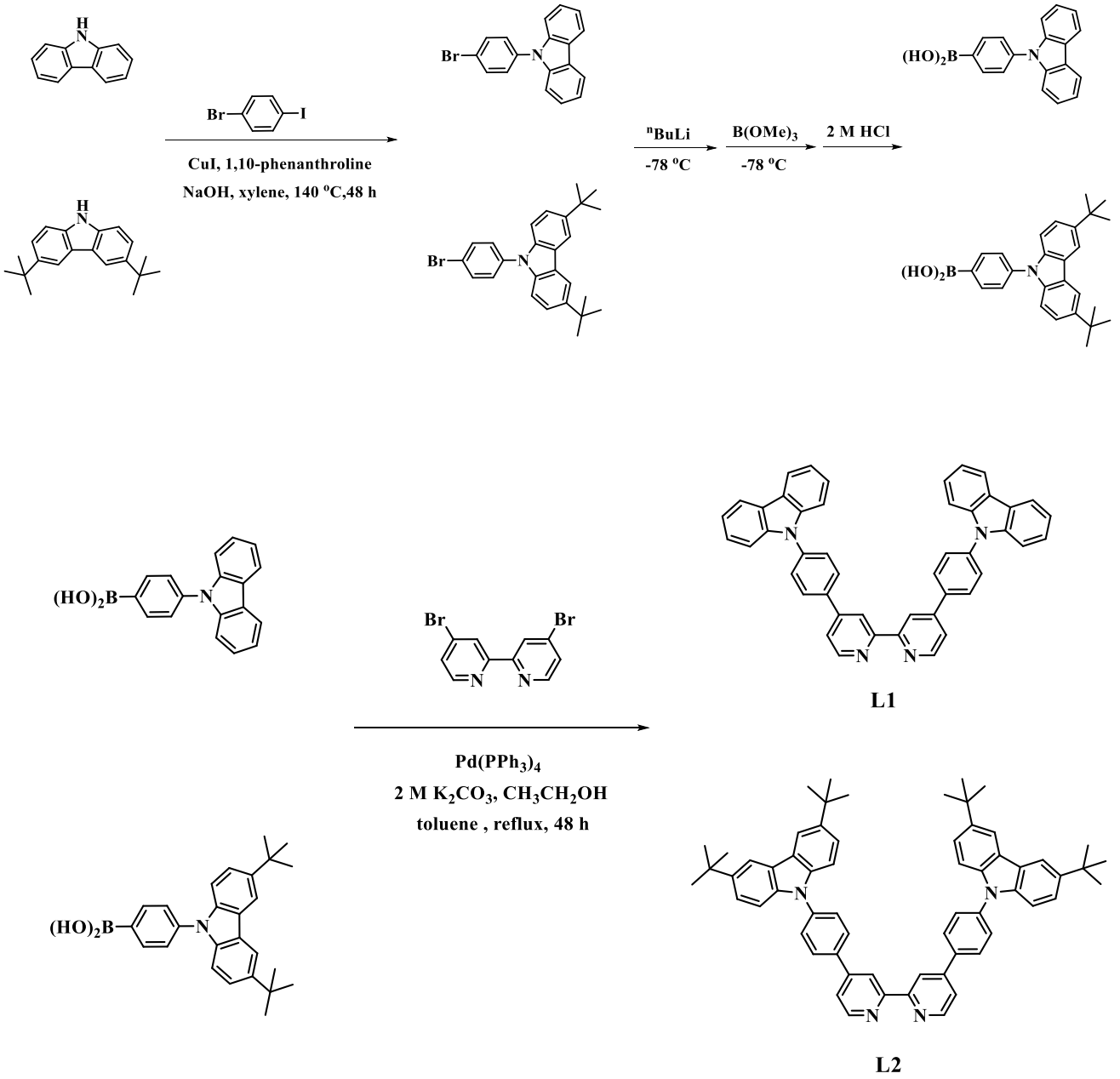

Scheme 1 Synthetic routes for ligands **L1–L2**

For compounds **E1** and **E2**, they exhibited similar emission spectra at room temperature and even 77 K, implying that the introduction of *t*-butyl groups on the carbazole moiety in bipyridine ligand have no impact on their emission energy. Without regard to the emission, these t-butyl groups could prevent the intermolecular π–π stacking and improve the solubility of the complex. However, these two complexes were significantly blue-shifted at 77 K with respect to their emission spectra at room temperature. These hypsochromic shifts resulted from the solvent reorganization. For complex **E3**, the emission maximum at 77 K was located at 471 nm with a shoulder peak at 502 nm. Upon freezing, the light emission may come from a mixing of ligand-centered $^3\pi$–π^* transition and ^{3}MLCT state [22, 23]. Therefore, a fine structured emission spectrum was observed here.

At 77 K in a rigid matrix, compounds **E4–E6** also displayed a vibronic structured emission spectra, confirming that they possessed dominant ^{3}MLCT excited states in preference to the ligand-centered $^3\pi$–π^* transitions [24]. Interestingly, these compounds containing the same C^N ligand (2-phenylisoquinoline) exhibited resembling emission band shapes with λ_{max} at 580 nm and a shoulder at

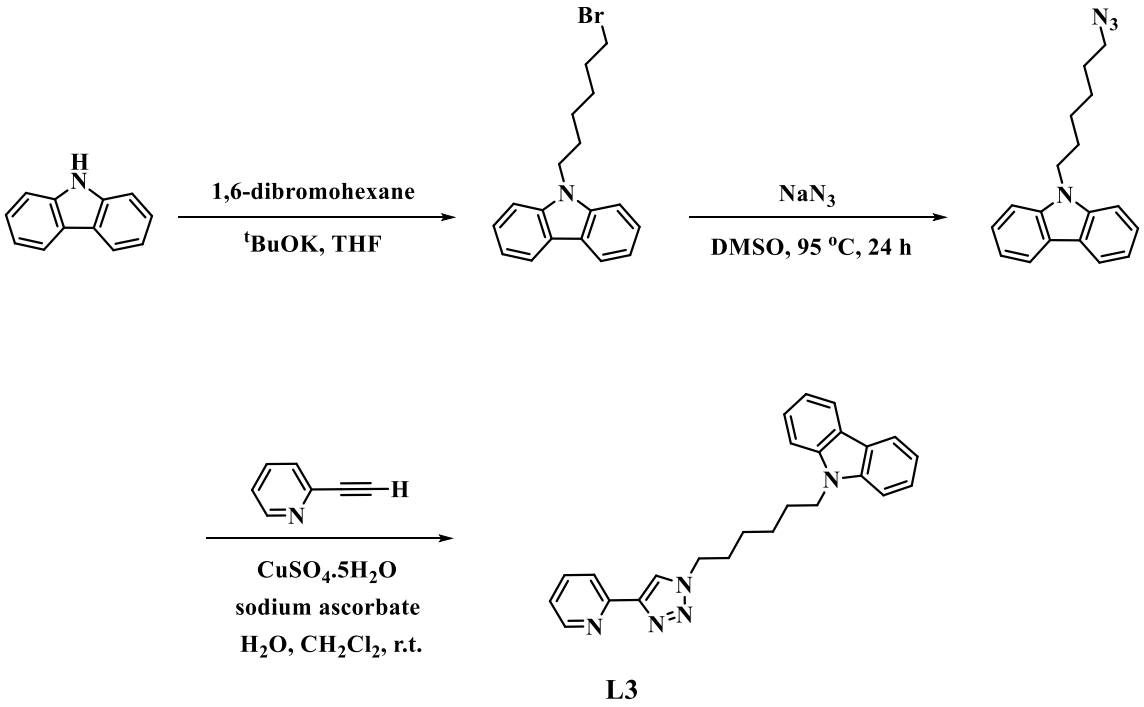

Scheme 2 Synthetic routes for ligand **L3**

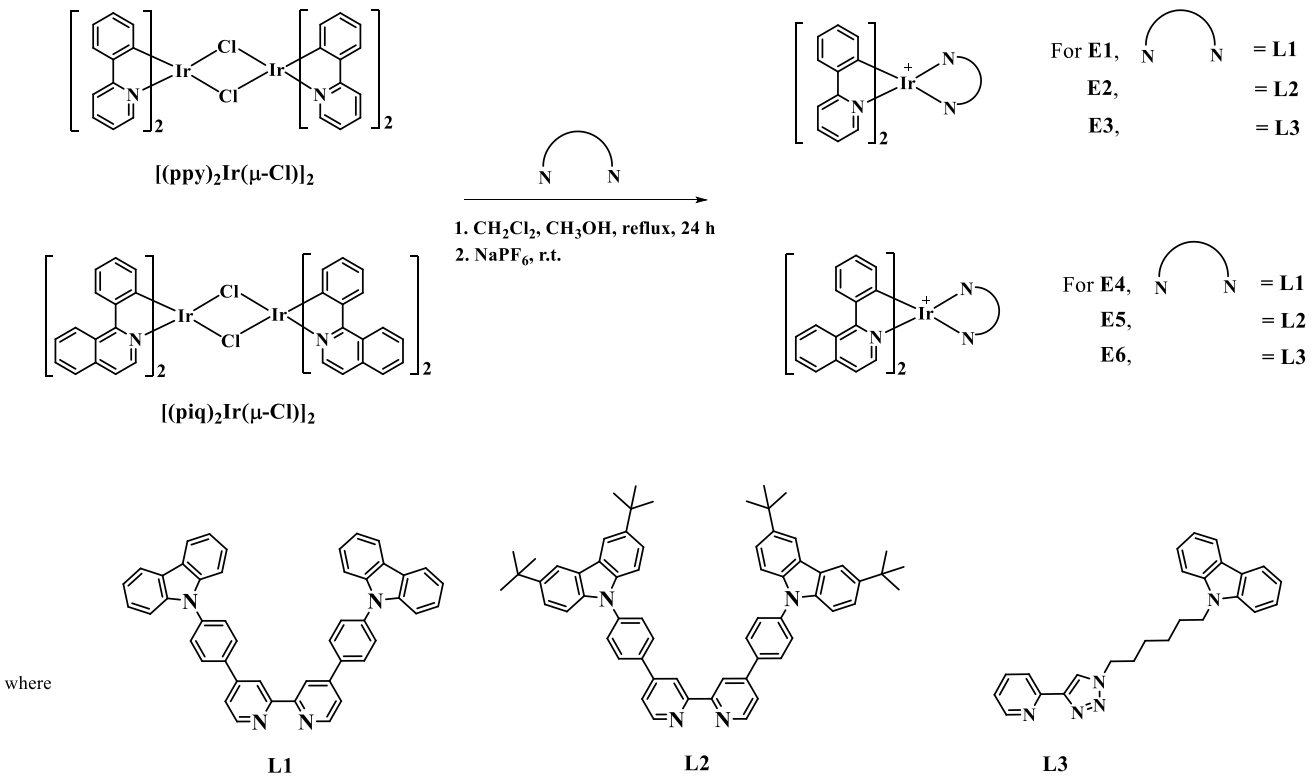

Scheme 3 Synthetic routes for complexes **E1–E6**

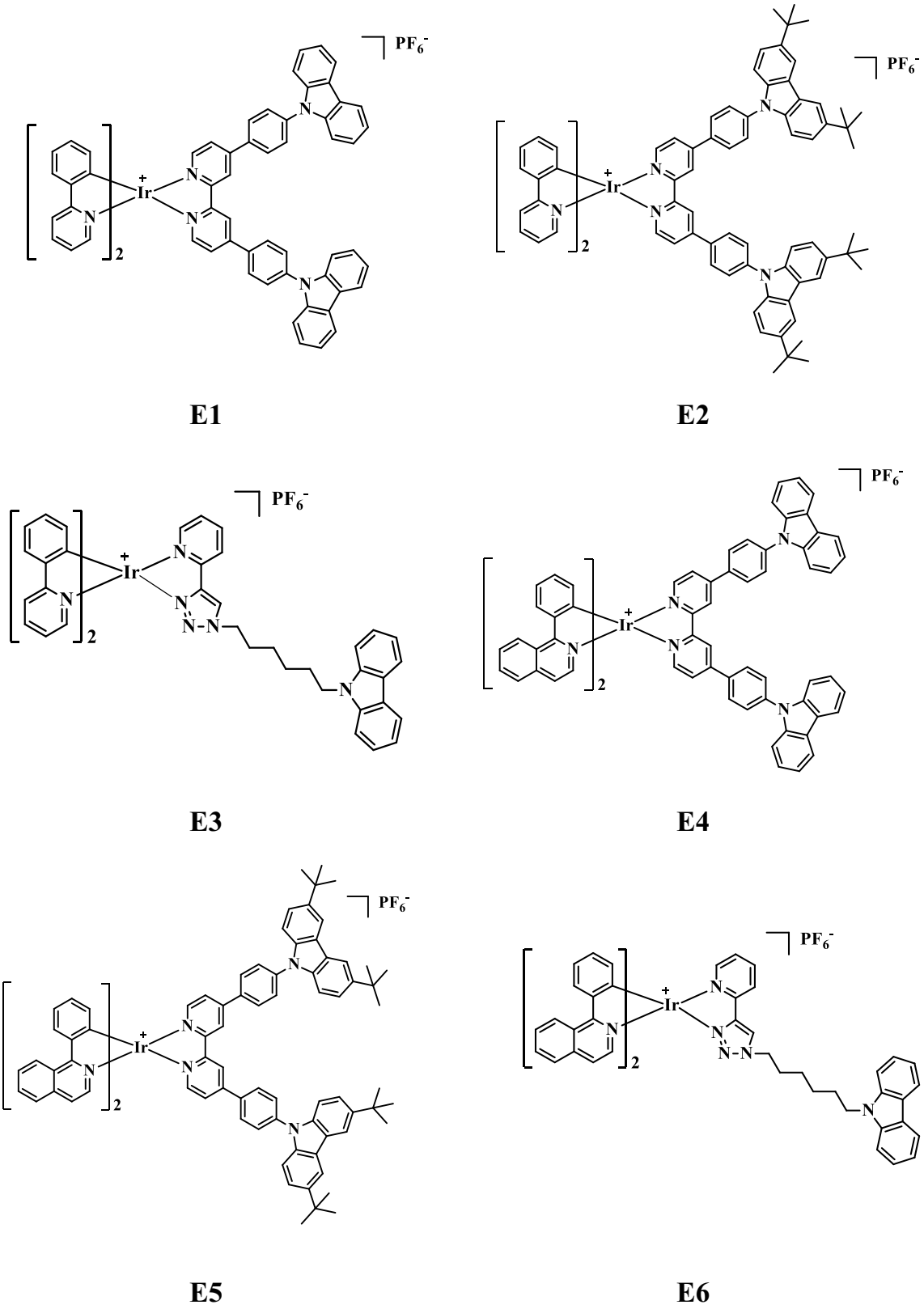

Fig. 1 Molecular structures of complexes **E1–E6**

Table 1 Photophysical data of complexes **E1–E6**

Complex	λ_{abs} [nm] (ε, 10^4 M^{-1} cm^{-1})	PL 298 K λ_{max} [nm][a]	PL 77 K λ_{max} [nm][a]	Φ_P
E1	289 (4.3), 338 (2.0), 393 (1.7)	598	536	0.11
E2	295 (4.2), 345 (1.8), 409 (1.5)	600	531	0.14
E3	263 (3.3), 294 (1.7), 385 (0.3)	506	471, 502sh	0.18
E4	292 (4.2), 339 (1.0), 384 (0.8)	594	581, 628sh	0.07
E5	295 (3.9), 346 (1.9), 414 (1.2)	604, 617sh	581, 626sh	0.09
E6	264 (3.4) 294 (3.4) 364 (1.3)	604	580, 627sh	0.11

[a] Measured in CH_2Cl_2 at 298 K, extinction coefficients (10^4 M^{-1} cm^{-1}) are shown in parentheses. sh = shoulder peak

[b] Measured in degassed CH_2Cl_2 at 298 K relative to *fac*-Ir(ppy)$_3$ ($\Phi_P = 0.40$), $\lambda_{ex} = 400$ nm

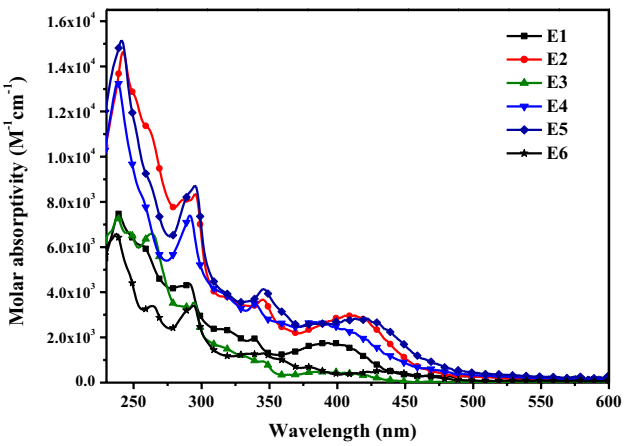

Fig. 2 UV–Vis absorption of complexes **E1–E6** in CH_2Cl_2 at 298 K

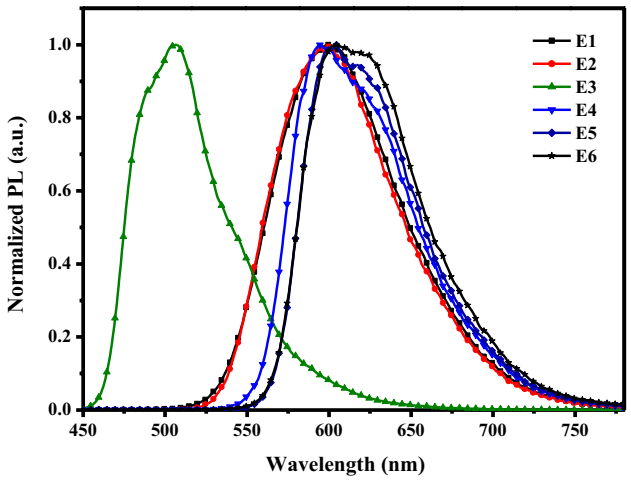

Fig. 3 Normalized PL spectra of complexes **E1–E6** in CH_2Cl_2 at 298 K

629 nm. It is considered that the emission from these three complexes at 77 K was attributed to the interaction between metal center and 2-phenylisoquinoline rather than the N,N′-ligands (**L1-L3**).

Furthermore, the photoluminescence quantum yields (Φ_P) of these six compounds were measured in degassed dichloromethane solutions with the excitation wavelength at 400 nm. The benchmark *fac*-Ir(ppy)$_3$ was used as the reference standard ($\Phi_P = 0.40$). The results are listed in the Table 1.

3.3 Electrochemical Properties

The electrochemical properties of these complexes **E1–E6** were examined by cyclic voltammetry. Ferrocenium/ferrocene (Fc/Fc^+) couple was employed as the internal standard. All these compounds were dissolved in tetrahydrofuran solution whereas 0.1 M tetrabutylammonium hexafluorophosphate was used as the supporting electrolyte. The apparatus for measurement equipped with a glassy carbon working electrode, a platinum wire counter electrode as well as a Ag/Ag^+ reference electrode was used. The electrochemical

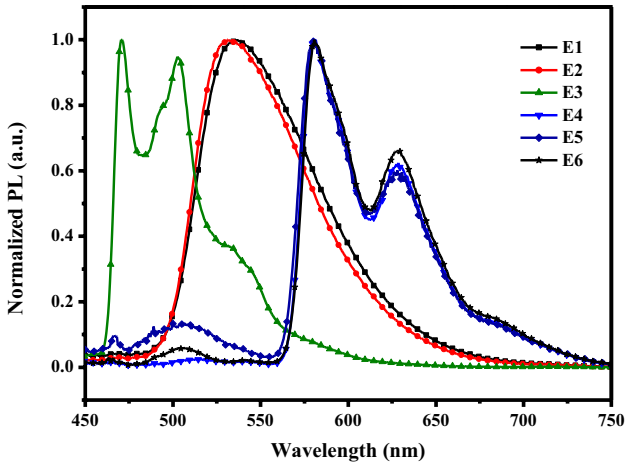

Fig. 4 Normalized PL spectra of complexes **E1–E6** in CH_2Cl_2 at 77 K

performances of **E1–E6** are summarized in Table 2. Their onset of redox potentials were recorded. The HOMO and LUMO energy levels were calculated from their corresponding oxidation and reduction potentials independently.

It is well understood that the energy gap of the iridium(III) complexes can be fine-tuned by modifying the molecular structure of the ligand [25]. On the whole, the HOMO is localized on the d-orbitals of the central iridium ion and the π-orbitals of the phenyl part in the cyclometalating ligands whereas the LUMO is predominantly dispersed on the pyridine ring in the ligand [26].

For the iridium(III) complexes, they underwent a reversible oxidation wave in the range of 0.74 and 0.84 V, which originated from the Ir(III)/Ir(IV) oxidation. On the other hand, these compounds showed an irreversible reduction wave under a cathodic sweep. Their reduction potentials ranged from − 1.32 to − 1.58 V.

With regard to the preceding CV studies on the cationic iridium(III) complexes, the reduction potential is mainly attributed to the reduction capability of the N^N ligand [27, 28]. In this case, the complexes **E3** and **E6** with ligand **L15** have more negative reduction potentials. Compared to the other compounds **E1–E2** and **E4–E5**, the pyridyl-1,2,3-triazole ligand in **E3** and **E6** made the reduction potentials less positive and then destabilized their LUMO levels. Furthermore, considering the C^N ligands in the complexes, compounds **E4–E6** bearing 2-phenylisoquinoline ligands have less negative reduction potentials than **E1–E3** consisting of 2-phenylpyridine.

3.4 Thermal Properties

The thermal stabilities of these charged complexes **E1–E6** were gauged by thermogravimetric analysis. The decomposition temperature at 5% weight-loss ranges from 324 to 393 °C, indicating that they are thermally stable upon heating to 300 °C. Based on the nature of coordination complexes, diamine ligand will dissociate from the metal atom in the first place. Compounds **E1** and **E4** as well as **E2** and **E5** exhibited similar 5%-weight loss temperature, suggestive of the dissociation of their N,N′-bipyridine ligands (Fig. 5 and Table 3).

3.5 Aggregation-Induced Emission Enhancement Properties

Aggregation-induced emission enhancement (AIEE) is a phenomenon in which the substance is weakly emissive or almost non-emissive in solution but very emissive in the aggregate or solid state. In 2001, Tang et al. reported that the luminescence of an organic fluorophore was stronger in the aggregate state than that in the solution state [29, 30]. This phenomenon is called "Aggregation-Induced Emission" (AIE). After this, many researchers have devoted their efforts to construct the materials with AIE properties since aggregation-caused quenching (ACQ) will deteriorate the OLED performance [31, 32]. In 2002, Park and co-workers reported that the nanoparticles exhibited enhanced fluorescence

Table 2 Electrochemical studies of complexes **E1–E6**

Complex	E_{ox} [V][1]	E_{red} [V][1]	HOMO [eV][2]	LUMO [eV][3]	E_g [eV][4]
E1	0.74	− 1.47	− 5.54	− 3.33	2.21
E2	0.84	− 1.45	− 5.64	− 3.35	2.29
E3	0.76	− 1.58	− 5.56	− 3.22	2.34
E4	0.80	− 1.32	− 5.60	− 3.48	2.12
E5	0.83	− 1.34	− 5.63	− 3.46	2.17
E6	0.80	− 1.46	− 5.60	− 3.34	2.26

[1] Obtained from the onset potential

[2] HOMO = − 4.8–E_{ox}

[3] LUMO = − 4.8–E_{red}

[4] E_g = LUMO–HOMO

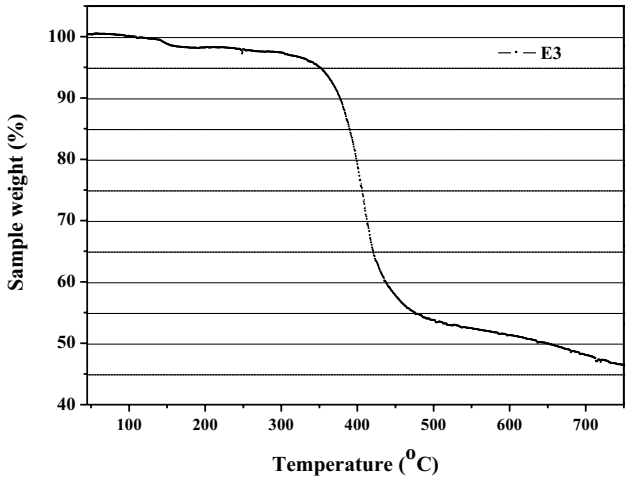

Fig. 5 A plot of weight % versus temperature for complex **E3**

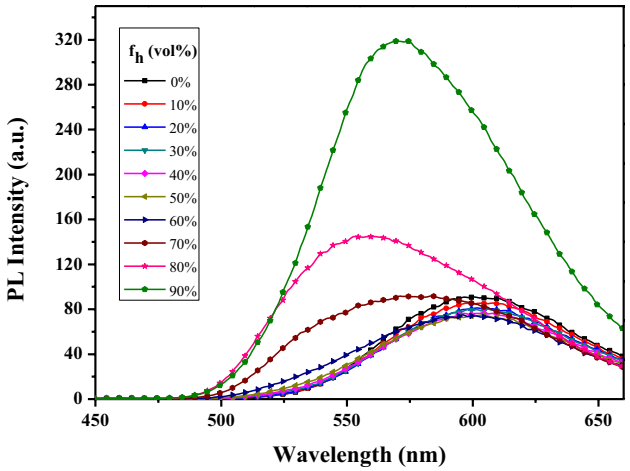

Fig. 6 Emission spectra of **E2** in $CHCl_3$/hexane mixture with different hexane fractions (0–90%)

Table 3 Thermal studies of complexes **E1–E6**

Complex	T_d [°C][1]	Complex	T_d [°C][1]
E1	351	**E4**	351
E2	391	**E5**	393
E3	350	**E6**	324

[1] Temperature at 5% weight loss

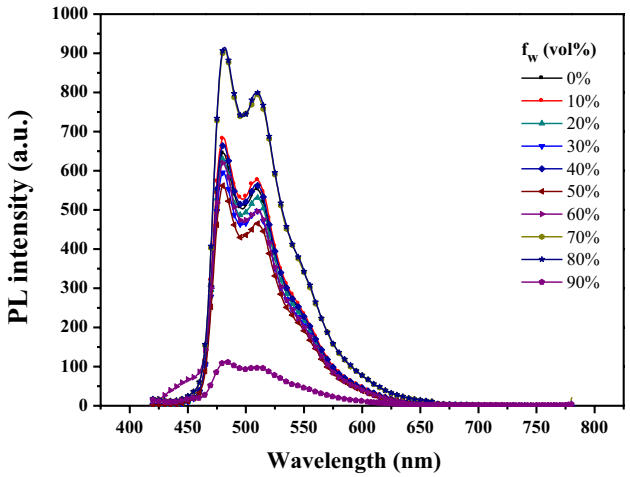

Fig. 7 Emission spectra of **E3** in THF/H_2O mixtures with different water fractions (0–90%)

emission, defining aggregation-induced emission enhancement (AIEE) [33].

Interestingly, two compounds **E2** and **E3** exhibited very weak emission in solution, but more intense emission in the aggregated state. With regard to these characteristics, these complexes are expected to perform AIEE behavior.

For the sake of investigating their AIEE features, different types of solvent systems were used. Upon excitation at 380 nm, their AIEE properties were studied by photoluminescence spectroscopy.

For complex **E2**, different portions of hexane, a poor solvent for this compound, were gradually added to the chloroform solutions with the hexane fractions (f_h) of 0–90%. The concentration was kept at 3.0×10^{-5} mol/L. The emission intensity increased dramatically when the hexane content was up to 90%. The emission maximum shifted from 600 to 569 nm and the color changed from weak orange to strong yellow (Fig. 6).

As for complex **E3**, it is very soluble in tetrahydrofuran but insoluble in water. After addition of water into the THF solution, the compound became aggregated. The PL emission was very weak when the water content was below 70%. Then the luminescence intensity was remarkably enhanced when the water content reached 70% (Fig. 7).

This phenomenon is explained by the restriction of molecular rotation. The larger structural relaxation as well as weakly emissive excited-state intraligand charge transfer (^{3}ILCT) features are responsible for the non-emission in solution [34]. In the solid state, the non-radiative processes like molecular rotation and vibration, are forcefully restricted [35, 36]. Based on the pioneering works, the ^{3}ILCT can enrich the iridium(III) compounds with AIE properties to a certain extent.

For the AIEE-active compound, this aggregation leads to less vibrational motion, resulting in the suppression of the rate of non-radiative decay. The emission is intensely enhanced owing to the restriction of intramolecular rotation of the ligand in the complex. Then it will prevent the energy loss from the non-radiative decay and more energy will be reserved for light emission.

3.6 Device Performance

The electroluminescence properties of these iridium(III) complexes were investigated. A series of doped multilayer OLEDs with configurations of ITO/PEDOT (indium tin oxide/poly(3,4-ethylenedioxythiophene, 40 nm)/PVK:OXD-7:compound (poly(*N*-vinylcarbazole)-1,3-bis[2-(4-tert-butylphenyl)-1,3,4-oxadiazo-5-yl]benzene–metal complex, (7:3:x wt%))/TmPyPb (1,3,5-tri[(3-pyridyl)-phen-3-yl] benzene, 50 nm)/LiF (1 nm)/Al (100 nm) were fabricated in which PEDOT was employed as a hole-injection layer and to smooth the ITO surface. PVK was used as the electron-blocking layer to accomplish the charge balance in the emissive layer [37] whereas OXD-7 acts as the electron-transporting material [38].

As summarized in Table 4, the devices based on compounds **E1–E6** were optimized. All of the devices **D1–D3** containing 2-phenylpyridine ligands showed better efficiencies than those **D4–D6** bearing 2-phenylisoquinoline ligands. Device **D1** based on complex **E1** exhibited maximum luminance (L_{max}) of 26,800 cd/m^2, current efficiency ($\eta_{L,\,max}$) of 35.0 cd/A and power efficiency ($\eta_{P,\,max}$) of 18.5 lm/W, which was much higher than device **D2** based on complex **E2**. As shown in Fig. 8, the device **D1** gave a greenish yellow emission peaking at 535 nm with the CIE coordinates of (0.38, 0.56), which was significantly blue-shifted than **D2**. It was noteworthy that the device **D1** exhibited a small efficiency roll-off and maintained current efficiencies of 33.4 and 30.8 cd/A, respectively at 100 and 1000 cd/m^2. This may be attributed to the sufficient triplet energy levels between Ir(ppy) core and ligand **L1** resulting in a complete energy transfer within the complex. However, the poor solubility of complex **E1** is not beneficial for device fabrication. Complex **E2** bearing two *tert*-butyl groups on 3,6-position of 9-phenyl-9*H*-carbazole moieties in the device **D2** can improve the solubility itself and tune the energy band gap. It showed a yellow emission with a maximum at 555 nm, L_{max} of 39,200 cd/m^2, current efficiency ($\eta_{L,\,max}$) of 27.7 cd/A and power efficiency ($\eta_{P,\,max}$) of 11.7 lm/W (Fig. 9).

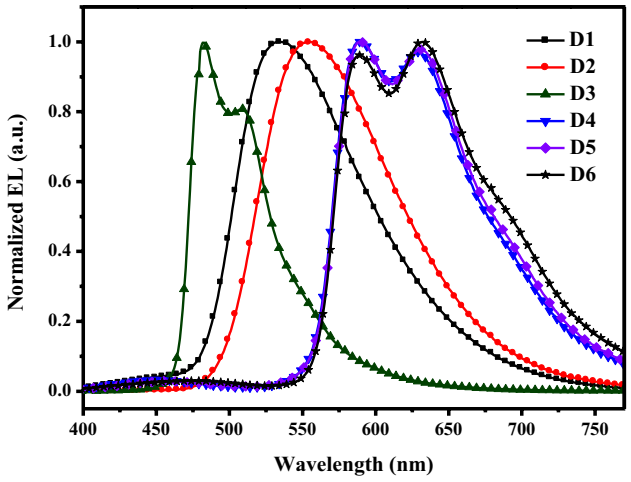

Fig. 8 Normalized EL spectra of the devices **D1–D6**

4 Concluding Remarks

Aggregation in the solid state causes self-quenching, which deteriorate the OLED performance. As mentioned above, the charged iridium(III) complexes reported by Su and co-workers exhibited AIE properties, which could overcome the problems on aggregation-caused quenching. In order to suppress the triplet–triplet annihilation and π–π stacking, some bulky ancillary ligands were introduced into our cationic iridium(III) complexes and their EL performance was investigated.

Most compounds except **E3** showed red emission at room temperature and significantly blue-shifted bands at 77 K in the solid matrices. Interestingly, compounds **E2** and **E3** showed AIEE properties. They were weakly emissive in the "good" solvent. The addition of "poor" solvent resulted in strong emission. As is known, it is difficult to obtain the charged metal complexes with good EL performance. It was found that attaching the bulky groups on the ancillary ligand can alleviate the problems of self-quenching in the solid state and improve the solubility of

Table 4 EL performance of the charged Ir(III) complexes.[a]

	λ_{em} [nm]	V_{on} [V]	L_{max} [cd/m^2]	$\eta_{L,\,max}$ [cd/A]	$\eta_{P,\,max}$ [lm/W]	CIE [x, y]
E1 (7 wt%)	535	4.8	26,800	35.0	18.5	(0.38, 0.56)
E2 (5 wt%)	555	6.0	39,200	27.7	11.7	(0.44, 0.54)
E3 (5 wt%)	484sh, 512	4.0	19,180	22.5	14.0	(0.18, 0.48)
E4 (2 wt%)	590, 631sh	5.8	7800	9.4	4.6	(0.59, 0.39)
E5 (1 wt%)	592, 632sh	4.8	8350	10.3	6.0	(0.60, 0.39)
E6 (5 wt%)	590sh, 632	5.0	5305	8.5	4.6	(0.60, 0.38)

[a] V_{on} is the turn-on voltage at 1 cd/m^2, L_{max} is the maximum luminance, $\eta_{L,\,max}$ and $\eta_{P,\,max}$ is the maximum current efficiency and power efficiency, respectively. CIE is the Commission International de l'eclairage Coordinates

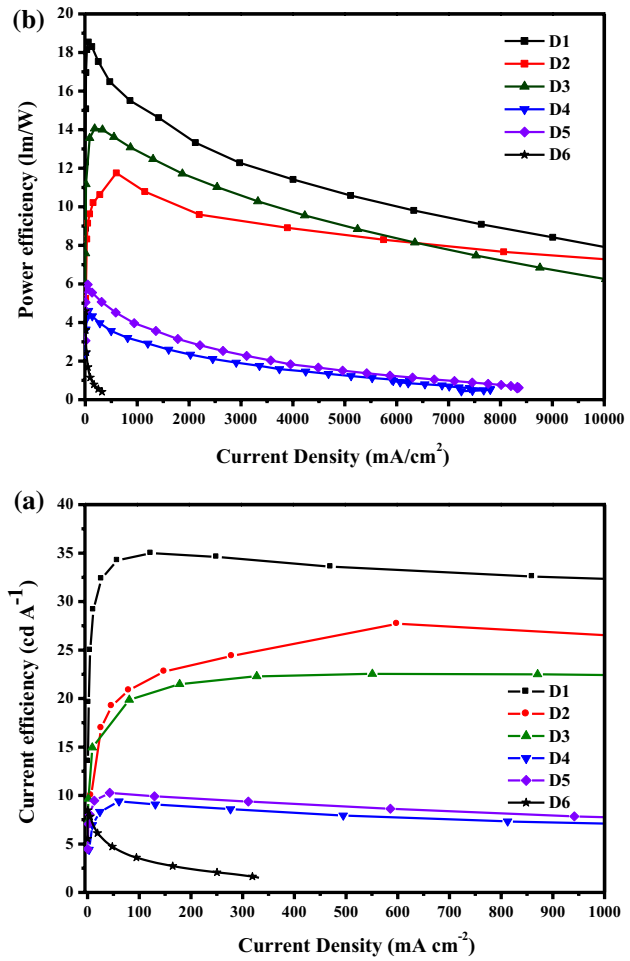

Fig. 9 Variation of (**a**) current efficiency and (**b**) power efficiency with current density in devices **D1–D6**

the complex. Among these charged metal complexes, **E1** exhibited L_{max} of 26,800 cd/m^2, $\eta_{L,\,max}$ of 35.0 cd/A and $\eta_{P,\,max}$ of 18.5 lm/W with a small efficiency roll-off suggesting that introducing the bulky moieties would alter the device efficiency significantly.

Acknowledgements W.-Y. W. thanks the financial support from the National Key R&D Program of China (2022YFE0104100), National Natural Science Foundation of China (52073242), ITC Guangdong-Hong Kong Technology Cooperation Funding Scheme (TCFS) (GHP/038/19GD), CAS-Croucher Funding Scheme for Joint Laboratories (ZH4A), the Hong Kong Research Grants Council (PolyU 15301922), Miss Clarea Au for the Endowed Professorship in Energy (847S) and Research Institute for Smart Energy (CDAQ). Q. W. and J. L. thank the financial support from Chengdu University.

Author Contributions Wai-Yeung Wong: funding acquisition, project administration, resources, supervision, writing-original draft, review & editing; Nga-Yuen Chau: conceptualization, investigation, writing-original draft; Qiwei Wang: data curation, investigation; Lu Jiang: data curation, investigation; Junlong Li: data curation, investigation; Zelin Sun: data curation, investigation.

Funding Open access funding provided by The Hong Kong Polytechnic University

Declarations

Competing Interests The authors declare no competing interests.

References

1. D. Tanaka, H. Sasabe, Y.-J. Li, S.-J. Su, T. Takeda, J. Kido, Jpn. J. Appl. Phys. **46**, L10 (2007)
2. M.G. Helander, Z.B. Wang, J. Qiu, M.T. Greiner, D.P. Puzzo, Z.W. Liu, Z.H. Lu, Science **332**, 944–947 (2011)
3. F. Kessler, Y. Watanabe, H. Sasabe, H. Katagiri, M.K. Nazeeruddin, M. Grätzel, J. Kido, J. Mater. Chem. C **1**, 1070–1075 (2013)
4. S. Lee, S.-O. Kim, H. Shin, H.-J. Yun, K. Yang, S.-K. Kwon, J.-J. Kim, Y.-H. Kim, J. Am. Chem. Soc. **135**, 14321–14328 (2013)
5. M.S. Lowry, S. Bernhard, Chem. Eur. J. **12**, 7970–7977 (2006)
6. B. Whittle, N.S. Everest, C. Howard, M.D. Ward, Inorg. Chem. **34**, 2025–2032 (1995)
7. K.K.-W. Lo, W.-K. Hui, C.-K. Chung, K.H.-K. Tsang, D.C.-M. Ng, N. Zhu, K.-K. Cheung, Coord. Chem. Rev. **249**, 1434–1450 (2005)
8. F. Monti, F. Kessler, M. Delgado, J. Frey, F. Bazzanini, G. Accorsi, N. Armaroli, H.J. Bolink, E. Ortí, R. Scopelliti, M.K. Nazeeruddin, E. Baranoff, Inorg. Chem. **52**, 10292–10305 (2013)
9. M.A. Baldo, C. Adachi, S.R. Forrest, Phys. Rev. B **75**, 125328 (2007)
10. N.C. Giebink, S.R. Forrest, Phys. Rev. B **77**, 235215 (2008)
11. X.G. Hou, Y. Wu, H.-T. Cao, H.-Z. Sun, H.-B. Li, G.-G. Shan, Z.-M. Su, Chem. Commun. **50**, 6031–6034 (2014)
12. G.-G. Shan, H.-B. Li, H.-Z. Sun, D.-X. Zhu, H.-T. Cao, Z.-M. Su, J. Mater. Chem. C. **1**, 1440–1449 (2013)
13. C.-L. Ho, Q. Wang, C.-S. Lam, W.-Y. Wong, D. Ma, L. Wang, Z.-Q. Gao, C.-H. Chen, K.-W. Cheah, Z. Lin, Chem. Asian J. **4**, 89–103 (2009)
14. S. Liu, P. Muller, M.K. Takase, T.M. Swager, Inorg. Chem. **50**, 7598–7609 (2011)
15. F. Himo, T. Lovell, R. Hilgraf, V.V. Rostovtsev, L. Noodleman, K.B. Sharpless, V.V. Fokin, J. Am. Chem. Soc. **127**, 210–216 (2005)
16. D.M. Nguyen, D.H. Miles, Synth. Commun. **41**, 1759–1771 (2011)
17. C. Ulbricht, B. Beyer, C. Friebe, A. Winter, U.S. Schubert, Adv. Mater. **21**, 4418–4441 (2009)
18. F. Neve, A. Crispini, Eur. J. Inorg. Chem. 1039–1043 (2000).
19. F. Neve, A. Crispini, S. Campagna, S. Serroni, Inorg. Chem. **38**, 2250–2258 (1999)

20. A.B. Tamayo, S. Garon, T. Sajoto, P.I. Djurovich, I.M. Tsyba, R. Bau, M.E. Thompson, Inorg. Chem. **44**, 8723–8732 (2005)
21. S. Sprouse, K.A. King, P.J. Spellane, R.J. Watts, J. Am. Chem. Soc. **106**, 6647–6653 (1984)
22. S. Lamansky, P. Djurovich, D. Murphy, F. Abdel-Razzaq, H.-E. Lee, C. Adachi, P.E. Burrows, S.R. Forrest, M.E. Thompson, J. Am. Chem. Soc. **123**, 4304–4312 (2001)
23. Y.-Y. Lyu, Y. Byun, O. Kwon, E. Han, W.S. Jeon, R.R. Das, K. Char, J. Phys. Chem. B **110**, 10303–10314 (2006)
24. W.-Y. Wong, G.J. Zhou, X.M. Yu, H.S. Kwok, B.Z. Tang, Adv. Funct. Mater. **18**, 928–937 (2008)
25. S.O. Jung, Y. Kang, H.S. Kim, Y.H. Kim, C.L. Lee, J.J. Kim, S.K. Kwon, Eur. J. Inorg. Chem. **17**, 3415–3423 (2004)
26. P.J. Hay, J. Phys. Chem. A **6**, 1634–1641 (2002)
27. H.C. Su, F.C. Fang, T.Y. Hwu, H.H. Hsieh, H.F. Chen, G.H. Lee, S.M. Peng, K.T. Wong, C.C. Wu, Adv. Funct. Mater. **17**, 1019–1027 (2007)
28. B. Chen, Y. Li, W. Yang, W. Luo, H. Wu, Org. Electron. **12**, 766–773 (2011)
29. J.D. Luo, Z.L. Xie, J.W.Y. Lam, L. Cheng, H.Y. Chen, C.F. Qiu, H.S. Kwok, X.W. Zhan, Y.Q. Liu, D.B. Zhu, B.Z. Tang, Chem. Commun. **18**, 1740–1741 (2001)
30. Y. N. Hong, J. W. Y. Lam, B. Z. Tang, Chem. Commun. 4332–4353 (2009)
31. G.G. Shan, D.X. Zhu, H.B. Li, P. Li, Z.M. Su, Y. Liao, Dalton Trans. **40**, 2947–2953 (2011)
32. K. W. Huang, H. Z. Wu, M. Shi, F. Y. Li, T. Yi, C. H. Huang, Chem. Commun. 1243–1245 (2009).
33. B.-K. An, S.-K. Kwon, S.-D. Jung, S.Y. Park, J. Am. Chem. Soc. **124**, 14410–14415 (2002)
34. Y. Wu, H.-Z. Sun, H.-T. Cao, H.-B. Li, G.-G. Shan, Y.-A. Duan, Y. Geng, Z.-M. Su, Y. Liao, Chem. Commun. **50**, 10986–10989 (2014)
35. N. Zhao, Y.H. Wu, L.X. Shi, Q.P. Lin, Z.N. Chen, Dalton Trans. **39**, 8288–8295 (2010)
36. N. Zhao, Y.H. Wu, H.M. Wen, X. Zhang, Z.N. Chen, Organometallics **28**, 5603–5611 (2009)
37. J.-W. Lee, J.-K. Kim, Y.-S. Yoon, Chin. J. Chem. **28**, 115–118 (2010)
38. Y. Xu, R. Yang, J. Peng, A.A. Mikhailovsky, Y. Cao, T.-Q. Nguyen, G.C. Bazan, Adv. Mater. **21**, 584–588 (2009)